# Alumina Nanofibers Grafted with Functional Groups: A New Design in Efficient Sorbents for Removal of Toxic Contaminants from Water

Dongjiang Yang[a], Blain Paul[a], Wujun Xu[b], Yong Yuan [a], Erming Liu [a], Xuebin Ke [a], Robert M. Wellard [a], Cheng Guo[c], Yao Xu[b], and Yuhan Sun[b] Huaiyong Zhu[a,*],

[*]Corresponding author. E-mail: hy.zhu@qut.edu.au

[a] School of Physical and Chemical Sciences, Queensland University of Technology, Brisbane, Qld 4001, Australia,

[b] State Key Laboratory of Coal Conversion, Institute of Coal Chemistry, Chinese Academy of Sciences, Taiyuan 030001, China.

[c] College of Science, Nanjing University of Technology, Nanjing, China 21009.

**RECEIVED DATE (xxxx)**

**Abstract**

A new design in efficient sorbents for the removal of trace pollutants from water was proposed: grafting the external surface of γ-alumina (γ-$Al_2O_3$) nanofibers with functional groups that have a strong affinity to the contaminants. This new grafting strategy greatly improves the accessibility of these sorption sites to adsorbates and thus efficiency of the fibrous sorbents. The product sorbents could capture the pollutants selectively even when the concentration of the contaminants is extremely low. Two types of γ-$Al_2O_3$ nanofibers with different size were prepared via facile hydrothermal methods. Thiol groups were then grafted on the γ-$Al_2O_3$ fibers by refluxing the toluene solution of 3-mercpatopropyltrimethoxysilane (MPTMS). The thiol group modified fibers not only can efficiently remove heavy metal ions ($Pb^{2+}$ and $Cd^{2+}$) from water at a high flux, but also display high sorption capacity under sorption equilibrium conditions. Similar result was obtained from the nanofibers grafted with octyl groups which are employed to selectively adsorb highly diluted hydrophobic 4-nonylphenol molecules from water. This study demonstrates that grafting nanofibers is a new and effective strategy for developing efficient sorbents.

## 1. Introduction

Toxic inorganic or organic contaminants, such as heavy metal ions and alkylphenols, are serious threat to the health of a large population due to their high toxicity. One of the potential remedies to this problem is removal of the contaminants via a sorption process. Activated carbons (Clifford, D. et al., 1986; Huang, C. P. et al., 1989) and natural clays (Haderlein, S.B. et al., 1996; Weng, C. H. et al., 1997) have large surface areas, but display weak sorption ability due to their weak interaction with the target contaminants. Recent investigations have discovered that the sorption efficiency of porous inorganic materials, such as clays (Celis, R. et al., 2000; Lagadic, I. L. et al., 2001) and mesoporous silica (Feng, X. et al., 1997; Liu, J. et al., 1998; Mercier, L. et al., 1997; Brown, J. et al., 1999; Yoshitake, H. et al., 2004; Antochshuk, V. et al., 2003; Liu, A. M. et al., 2000), could be improved by grafting organic groups. These organic functional groups are grafted on the inorganic substrates via stable covalent bond and have strong affinity to certain class of toxic contaminants. Thus the grafted sorbents can capture the toxic contaminants selectively even if their concentration is extremely low. Currently the inorganic substrates possessing large specific surface area and numerous silanol groups are selected because large amount of functional groups (the capturers) can be grafted on these sorbents. For instance, montmorillonite and other smectite clays modified by quaternary ammonium compounds and/or thiols have been used to adsorb heavy metal ions from water. (Lagadic et al., 2001; Cody and Kemnetz 1997; Greco 1996; Mercier et al., 1998; Celis et al., 2000) Mesoporous silicas were also functionalized for the same purpose. *Liu* et al. (Feng, X. et al., 1997; Liu, J. et al., 1998) grafted thiol groups on the pore walls of MCM-41; *Pinnavaia* et al. (Mercier et al., 1997; Brown et al., 1999) achieved the covalent grafting of thiol moieties to HMS support; *Zhao* et al. (Liu et al., 2000) developed thiol- and amino-functionalized SBA-15 silicas. Furthermore, *Inumaru* et al. (Inumaru et al., 2000; Inumaru et al., 2004) used MCM-41 as support to make surface modification through grafting of alkyltriethoxysilane. The alkyl group grafted sorbents can selectively remove highly diluted alkylphenols from aqueous solution. However, there is a drawback when these porous substrates are grafted: The grafting substantially reduces the pore size, resulting in narrow and non-interconnected pores, and this restrains the flow of the solution through the

pores and constrains the adsorption efficiency of contaminants. Clearly, to undertake the sorption of heavy metal ions or organic pollutants, it is imperative to develop novel sorbents with large sorption capacity and enhanced sorption kinetics. The effective accessibility of grafted functional groups to the solution is the main focus for improving adsorption efficiency, and requires a radical change in the fundamental structure of the inorganic substrates.

In recent years, various oxide nanofibers have been reported (Xia et al., 2003; Zhu et al., 2004; Shen et al., 2007; Zhu et al., 2002; Zhu et al., 2004). Thin nanofibers possess large specific surface areas which enable large number of organic functional groups to be grafted; the voids between fibers are interconnected and much larger than the pores in clay based materials and mesoporous solids, allowing not only a higher flow rate but also giving the contaminants in the fluid more effective access to the grafted groups, hence better sorption. To verify the concept, two types of $\gamma$-$Al_2O_3$ nanofibers were used as substrates in the present study. Thiol and octyl groups were then grafted on the $\gamma$-$Al_2O_3$ fibers by refluxing the toluene solution of 3-mercpatopropyltrimethoxysilane (MPTMS) and n-octyltriethoxysilane (OTES), respectively. The large difference between the specific surface areas of the two substrates demonstrates the effect of the specific surface area on the performance of the functionalized fibers. As expected, the thiol grafted $\gamma$-$Al_2O_3$ fibers can efficiently adsorb $Pb^{2+}$ and $Cd^{2+}$ ions from water especially at a high water flux. Similarly, octyl grafted samples are well-proficient in selectively adsorbing highly diluted toxic 4-nonylphenol molecules from water. Obviously, the interconnected pore structure formed by the voids between the fibers makes the functional groups easier be accessed to target contaminants, and greatly improves the decontamination efficiency.

## 2. Experimental Section

**2.1. Preparation of $\gamma$-$Al_2O_3$ nanofibers.** Two types of $\gamma$-$Al_2O_3$ nanofibers with different size and surface area were prepared via hydrothermal method. The smaller fibers, FA(S), are 5-7 nm thick and 40 - 60 nm long and have a specific surface area of 290 $m^2g^{-1}$. They were synthesized by treating aluminum hydroxide precipitate with polyethylene oxide (PEO) surfactant (Tergitol 15S-7 from Aldrich) at 373K,

following the procedures reported in our previous studies (Zhu et al., 2002; Zhu et al., 2004). For instance, 18.8 g of $NaAlO_2$ (0.2 mol of Al) was dropped into 50 mL of 5 N acetic acid solution with vigorous stirring. The white precipitate was recovered by centrifugation and washed with deionized water four times to remove the sodium ions (pH= 4 ~ 5). PEO surfactant (40 g), with a general chemical formula $C_{12-14}H_{25-29}O(CH_2CH_2O)_7H$ and average molecular weight of about 508, was mixed with the washed aluminum hydrate cake. The sticky mixture was stirred for 4 h and then transferred into a closed autoclave and kept in an oven at 373 K. The molar ratio of $Al(OH)_3$:PEO:$H_2O$ in the mixture was 0.2:0.08:3.2. The autogenous pressure in the closed autoclave was about 1 atm. Fresh aluminum hydrate precipitate (prepared as described above and contain about 0.2 mol of $Al(OH)_3$) was added into the autoclaved mixture every 2 days. Accordingly, the molar ratio of $Al(OH)_3$:PEO:$H_2O$ changed to 0.4:0.08:6.4, 0.6:0.08:9.6, and 0.8:0.08:12.8, respectively, after 2, 4, and 6 days (post adding precipitate). The sample formed after 8 days displays typical fibrous morphology and has a crystal phase of boehmite. The obtained boehmite fibers were converted to γ-$Al_2O_3$ nanofibers by a calcination at 773 K. The larger fibers are ~10 nm thick and 300 nm long and have a specific surface area of 160 $m^2g^{-1}$. They were synthesized by employing the Bugosh procedure (Bugosh 1961), and converted to γ-$Al_2O_3$ nanofibers, FA(L) also by the calcination at 773 K.

**2.2. Grafting of functional groups.** Two silanes, 3-mercpatopropyltrimethoxysilane (MPTMS) and n-octyltriethoxysilane (OTES), were selected as coupling agents to graft functional thiol and octyl groups on the γ-$Al_2O_3$nanofibers by refluxing the suspension of the fibers, silanes and toluene.

For example, the thiol group grafted samples were prepared as follow: 0.6 mL (0.9 mL) of MPTMS was mixed with 1.5 g of FA(S) nanofibers in 50 mL of dried toluene. This mixture was stirred under reflux condition for 36 h. Then the solid in the mixture was collected by filtration, rinsed with anhydrous ethanol to remove the unreacted MPTMS and dried at 80 ºC for 24 h. The functionalized products were denoted as SH-FA(S)-1 (0.6 mL MPTMS) and SH-FA(S)-2 (0.9 mL MPTMS). Thiol groups were also grafted on larger γ-$Al_2O_3$ fibers obtained from Bugosh's approach in the same procedure. The samples were SH-FA(L)-1 and SH-FA(L)-2.

Similarly, the octyl group grafted samples were prepared as fellow: 1 mL (2 mL) of OTES was mixed with 1.0 g of FA(S) nanofibers in 50 mL of dried toluene. This mixture was stirred under reflux condition for 36 h. Then the solid in the mixture was collected by filtration, rinsed with anhydrous ethanol to remove the unreacted OTES and dried at 80 ºC for 24 h. The functionalized products were denoted as C8-FA(S)-1 (1 mL OTES) and C8-FA(S)-2 (2 mL OTES).

**2.3. Sorption experiments.** To study the sorption property of the thiol group grafted sorbents, two assessment methods were adopted. Firstly, to assess the sorption efficiency at a high flux, 100 mg of a sorbent was loaded in a glass column with diameter of 30 mm. 50 mL of aqueous solution with $Pb^{2+}$ (or $Cd^{2+}$) concentration of 50 parts per million (ppm) by mass, passed through the sorbent bed at flow rates of 10, 5, and 3 mL/min, respectively. Besides, to assess the sorption capacity of the sorbents, 10 mg portions of the functionalized sorbents were equilibrated with 50 mL volumes of lead nitrate solutions at initial concentrations ranging from 0 to 35 ppm for 18 h under shaking. For cadmium nitrate solutions, the initial concentrations range from 0 to 25 ppm. Sorption isotherms were generated by plotting the amount of toxic ions adsorbed per gram of sorbent (mmol $g^{-1}$) against the equilibrium concentration of the toxic ions in the 50 mL solution (i.e. the concentration after the 18 h shaking).

Octyl group grafted sorbents were designed to remove toxic 4-nonylphenol in aqueous solution. 50 mg of a sorbent was loaded in a glass column with diameter of 30 mm. 50 mL of aqueous solution with 4-nonylphenol concentration of 2 ppm by mass, passed through the sorbent bed at a flow rate of 10 mL/min.

After the sorption experiment, the supernatant solution was separated by centrifugation and millipore filter (0.45 μm) prior to the analysis. The change in heavy metal ion concentration was analyzed by inductively coupled plasma (ICP) technique using a Varian Liberty 200 ICP-OES. The residual 4-nonylphenol was analyzed with an ultraviolet (UV) spectrometer at 224 nm.

**2.4. Characterization.** TEM images were obtained using a Philips CM200 TEM or a FEI Tecnai 20 TEM with an accelerating voltage of 200 kV. The specimens were sample powders deposited onto a copper microgrid coated with a holey carbon film. Energy dispersive X-ray (EDX) attachment on FEI

Quanta 200 Environmental SEM was used to detect the elemental composition of the sorbents. X-ray diffraction (XRD) patterns of the sample powder were recorded on a Siemens D5000 diffractometer equipped with a graphite monochromator. Cu Kα radiation and a fixed power source (40 kV and 40 mA) were used. The data were collected over a $2\theta$ range between 4 and 75°, at a scanning rate of 2.5°/ min. $N_2$ adsorption/desorption isotherms of the samples were measured on a Micrometrics Tristar 3000 automated gas adsorption analyzer after the sample was pretreated at 110 °C under the flow of $N_2$ on a Micrometrics Flowprep 060 degasser. Specific surface area were calculated by using the BET equation and the isotherm data in a relative pressure ($P/P_0$) range between 0.05 and 0.2. Thermal decomposition of the samples was carried out in a high-resolution thermogravimetric analyzer (series Q500) of TA Instruments in a flowing nitrogen atmosphere (60 $cm^3$/min). Approximately 10 mg of specimen underwent thermal analysis, which was heated at a rate of 5 K/min to 1200 K.

## 3. Results

**3.1. XRD Patterns and FTIR Spectra.** The thiol and octyl groups grafted γ-$Al_2O_3$ nanofibers were measured by XRD and FTIR techniques. As shown in Fig. 1a, SH-FA(S)-1 and C8-FA(S)-1, thiol and octyl groups grafted small γ-$Al_2O_3$ nanofibers show XRD patterns of typical γ-alumina phase which is same as that of the inorganic parent substrate, indicating that the grafting did not affect the crystal structure of the fiber substrate. The FTIR spectra of the functionalized small γ-$Al_2O_3$ nanofibers were depicted in Fig. 1b. The band at 2550 $cm^{-1}$ is observed in the spectrum of SH-FA(S)-1, which is ascribed to the vibration of S-H bond (Lagadic et al., 2001). The bands in the 2850-2950 $cm^{-1}$ region are detected in the spectrum of C8-FA(S)-1, which are corresponding to the symmetric and antisymmetric C–H stretching vibration of $CH_3$ and $CH_2$. Additionally, the bands in the 1020-1090 $cm^{-1}$ region are observed in the grafted samples, which are assigned to the vibration of Si-O-Al bond (Farmer, 1974; Gadsden 1975). These facts indicate that the silane with thiol and octyle groups have been grafted on to the surface of γ-$Al_2O_3$ nanofibers, respectively.

**(Fig. 1 -** XRD patterns (a) and FTIR spectra (b) of the parent and functional group (thiol or octyl) grafted small γ-$Al_2O_3$ nanofibers.)

**3.2. SEM and TEM Images.** The morphology of the functionalized γ-$Al_2O_3$ nanofibers grafted with thiol or octyl group were observed from SEM and TEM images in Fig. 2. Fig. 2a is SEM image of SH-FA(L)-1. The thiol group grafted large γ-$Al_2O_3$ nanofibers were ~300 nm long and ~20 nm thick. The observed width of the fibers is larger than the real width because the sample was coated with a layer of gold (~5 nm thick) for the SEM measurement. Numerous interconnected mesoporous interparticle voids (10-20 nm) were found in the aggregation of randomly oriented nanofibers. For octyl group grafted small γ-$Al_2O_3$ nanofibers (Fig. 2c), the fibrous morphology was also preserved during the grafting processes. Similar mesoporous interparticle voids were observed. These interconnected mesoporous voids are important to the improvement of the sorption ability for toxic contaminants from water, heavy metal ions or organic 4-nonylphenol, because they could allow the contaminated water to pass through easily. TEM images and electron diffraction patterns (EDP) of SH-FA(L)-1 and C8-FA(S)-1 are displayed in Fig. 2b and d. The EDP images show that the grafted fibers present γ-alumina phase which is agreement with XRD result.

**(Fig. 2 -** SEM images of SH-FA(L)-1 (a). The observed width of the fibers is larger than the real width because the sample was coated with a layer of gold (~5 nm thick) for the SEM measurement. TEM image of SH-FA(L)-1 (b) and C8-FA(S)-1 (c). Inset: electron diffraction patterns (EDP) of SH-FA(L)-1 and C8-FA(S)-1.)

Additionally, the major composition of the grafted γ-$Al_2O_3$ nanofibers was detected by the EDX attachment of the SEM instrument. Atomic ratios of Si/Al for SH-FA(S)-1, SH-FA(S)-2, SH-FA(L)-1, SH-FA(L)-2, C8-FA(S)-1, and C8-FA(S)-2 are 1:9.1, 1:11.2, 1:17.8, 1:15.4, 1:13.7, and 1:12.1,

respectively. Obviously, more functional groups were grafted on the small nanofibers due to their large specific surface areas.

**3.3. $^{29}$Si NMR Spectra.** Fig. 3 shows the $^{29}$Si MAS NMR spectra of the samples SH-FA(S)-1, SH-FA(S)-2, C8-FA(S)-1, and C8-FA(S)-2. For thiol group grafted samples, all spectra exhibited distinct signals at -66 and -55 ppm (Fig. 3a), corresponding to $T^3$ $[(AlO)_3Si^*(CH_2)_3SH]$, and $T^2$ $[(CH_3CH_2O)(AlO)_2Si^*(CH_2)_3SH]$ environments of silicon atoms (Shimojima and Kuroda 2003), respectively. $T^1$ peak at ~40 ppm, which is assigned to $[(CH_3CH_2O)_2(AlO)_2Si^*(CH_2)_3SH]$ (Shimojima and Kuroda 2003) environment of silicon atom, was not observed. The ratios of $T^2/T^3$ silicon atoms were estimated from the ratio of $T^2/T^3$ peak area, being 3:1 and 5:1 for SH-FA(S)-1 and SH-FA(S)-2, respectively. The schematic representations of SH-FA(S)-1 and SH-FA(S)-2 in Fig. 3a (inset) are based on this information, where MPTES molecules are bound on the $\gamma$-$Al_2O_3$ nanofibers by condensation with two or three surface hydroxyl groups. For octyl group grafted samples (Fig. 3b), only $T^2$ $((CH_3CH_2O)(AlO)_2Si^*(CH_2)_7CH_3)$ environment of silicon atoms was detected from the spectra of C8-FA(S)-1 and C8-FA(S)-2. It means that every octyl molecule is grafted on the $\gamma$-$Al_2O_3$ nanofibers by condensation with two surface hydroxyl groups.

**(Fig. 3 -** Solid-state $^{29}$Si MAS NMR spectra of thiol (a) and octyl (b) grafted small $\gamma$-$Al_2O_3$ nanofibers. Inset: schematic conformations of functionalized layers on the surface of $\gamma$-$Al_2O_3$ nanofibers under different conditions.)

**3.4. $N_2$ Adsorption.** The $N_2$ adsorption-desorption isotherms and the pore size distributions (PSD) of the functionalised samples are shown in Fig. 4. The adsorption capacities by large fibres grafted with thiol groups were 0.67 $cm^3/g$, whereas that of the parent large $\gamma$-$Al_2O_3$ nanofibres was as high as 0.51 $cm^3/g$ (Fig. 4a). Given that adsorption strongly depends on the porosity of porous solids (Gregg and Sing 1982), surface grafting resulted in the reduction of pore volumes. The specific surface areas are 137 $m^2g^-$

[1] for SH-FA(L)-1 and 133 $m^2g^{-1}$ for SH-FA(L)-2, which are also lower than that of the parent support (160 $m^2g^{-1}$). The pore size distributions (PSDs) of the large γ-$Al_2O_3$ fibres and the thiol grafted samples were derived from the data of their nitrogen sorption isotherms and provided in Fig. 4b. Because the pores in the fibrous solids are the voids between nanofibres (Fig. 4a), which have irregular shapes and non-unifrom sizes, the PSD of pure large γ-$Al_2O_3$ fibres is broad and peaked at about 5.6 nm, as did the PSD of the grafted fibres. The results show that grafting reduced the volume of the voids between nanofibres moderately, but did not seriously affect the solution diffusion into these voids. Compared with parent small γ-$Al_2O_3$ fibres, the adsorption capacities of octyl group grafted samples reduced from 1.18 to 0.76 $cm^3/g$ (Fig. 4c); the specific surface areas of C8-FA(S)-1 and C8-FA(S)-2 are 244 and 234 $m^2g^{-1}$, being lower than that of the parent fibre (292 $m^2g^{-1}$). The PSDs of parent and grafted smaller γ-$Al_2O_3$ nanofibres all peaked at 15.7 nm. Similar results were obtained for thiol group grafted small fibres.

**(Fig. 4 -** Nitrogen sorption isotherms (a, c) and pore size distributions (b, d) based on the BJH model for thiol grafted large γ-$Al_2O_3$ nanofibers and octyl grafted small γ-$Al_2O_3$ nanofibers.)

**3.5. TGA Results.** The thermal gravimetric analysis (TGA) shows that the organic groups grafted on γ-$Al_2O_3$ nanofibers, thiol or octyl, are very stable. As shown in Fig. 5, a large weight loss related to the loss of thiol groups from the grafted fibers is observed at about 583 K, and the loss of octyl group from the grafted samples appears at a higher temperature. It indicates that the grafted MPTMS species are bonded strongly to the γ-$Al_2O_3$ fibers.

(**Fig. 5 -** TGA and DSC (inset) curves of SH-FA(S)-2 and C8-FA(S)-2.)

**3.6. Sorption for Heavy metal ions.** Considering that thiol group could adsorb heavy metal ions from water, the thiol grafted γ-$Al_2O_3$ nanofibers were employed to remove $Pb^{2+}$ and $Cd^{2+}$ ions. As shown in Fig. 6a, the pure γ-$Al_2O_3$ nanofibers FA(S) can remove 40% of $Pb^{2+}$ ions in solution and the $Pb^{2+}$ ion sorption does not change substantially when the flux varies. While the sorption abilities of the grafted nanofibers are much higher: SH-FA(S)-1 can remove 60, 67, and 74% of the $Pb^{2+}$ ion sorption at the flux of 10, 5, and 3 mL/min, respectively. SH-FA(S)-2 displays even better abilities to remove 82, 90, and 95% of the ions at the three flux rates, respectively, which are more than twice the sorption ability of the parent bare fibers. All the large nanofibers, FA(L), SH-FA(L)-1 and SH-FA(L)-2 exhibit lower removal ability, compared to the corresponding sorbents of small fibers. Similar results were also observed in the removal of $Cd^{2+}$ ions. For both large and small fibers, the common trend indicates that the more groups grafted on, the better the sorption ability.

The equilibrium sorption capacities of the sorbents were positively surprising. The isotherms of $Pb^{2+}$ ion sorption by the six sorbents are depicted in Fig. 6c. According to the isotherms the equilibrium sorption capacities (achieved after shaking for 18 h) of FA(S), SH-FA(S)-1, SH-FA(S)-2, FA(L), SH-FA(L)-1, and SH-FA(L)-2, are 0.15, 0.33, 0.37, 0.07, 0.19, and 0.22 mmol $g^{-1}$, respectively. For $Cd^{2+}$ ion sorption, the capacities are 0.07, 0.39, 0.42, 0.06, 0.18, and 0.21 mmol $g^{-1}$, respectively (Fig. 6d). Apparently, the thiol grafted fibrous sorbents not only exhibit super sorption ability for heavy metal ions at high flow rates, but also possess superior equilibrium sorption capacity.

(**Fig. 6 -** The performance and equilibrium sorption isotherms of thiol group grafted γ-$Al_2O_3$ nanofibers for removal $Pb^{2+}$ (a, c) and $Cd^{2+}$ ions (b, d) from aqueous solution. Sorption amounts were measured after a suspension of 10 mg of sorbent in 50 ml of $Pb^{2+}$ (or $Cd^{2+}$) solution was shaken at room temperature for 18 h. The concentration range of $Pb^{2+}$ is between 0 to 35 ppm, and that of $Cd^{2+}$ is between 0 to 25 ppm. For comparison, the sorption of the parent γ-$Al_2O_3$ nanofibers were also given.)

***(Table 1.*** The distribution coefficient $K_d$ (mL/g) in the presence and absence of $Na^+$ or $Ca^{2+}$ ions)

The selective sorption of the toxic cations by the sorbents was determined in the presence of $Na^+$ or $Ca^{2+}$ ions, and their concentrations were 400 to 1000 times that of the toxic ions. The sorption selectivity is expressed as the distribution coefficient $K_d$, which is the ratio of the amount (in milligram) of $M^{2+}$ ions absorbed by one gram of the sorbent to the amount of $M^{2+}$ remaining in solution (per milliliter) (Komarneni and Roy 1988; Nyman et al., 2001; Behrens et al., 1998). The coefficient was calculated from the equilibrium data (measured after 18 hour-stirring) and listed in Table 1. It can be found that the presence of large amount of $Na^+$ and $Ca^{2+}$ ions did not substantially reduce the sorption capacities of thiol grafted fibers for $Pb^{2+}$ and $Cd^{2+}$ ions. It means that the co-existed competitive cations only have slight influence on the sorption ability of the fibrous sorbents. These results suggest the grafted fibers are good sorbents for practical application where competitive ions exist.

**3.7. Hydrophobicity and Sorption for 4-nonylphenol.** Given the hydrophobic nature of the octyl groups, it is anticipated that octyl group grafted nanofibers are hydrophobic. The wettability was studied by measuring the contact angle (CA) of water on the surface of the tableted nanofibers. Fig. 7 shows the shape of a water-droplet on the surface of parent and octyl grafted small γ-$Al_2O_3$ nanofibers. The parent γ-$Al_2O_3$ nanofiber has a water CA of 21 ± 2º, displaying a hydrophilic trait (Fig. 7a). However, the thiol group grafted sample, C8-FA(S)-1, exhibits super hydrophobicity with a water CA of 145 ± 2º (Fig. 7b). The toxic 4-nonylphenol has a low solubility in aqueous solution due to its hydrophobic nonyl group. It is an endocrine disrupter from sewage disposal plants and shows its oestrogenic activity at very low concentrations (Preziosi 1998; Tyler and Routledge 1998; MuÜller and Schlatter 1998). To remove the highly diluted 4-nonylphenol molecules, molecular selectivity is crucial in sorption process. It has been reported that octyl group grafted silica-based mesoporous sorbents could selectively remove trace 4-nonylphenol from water. (Inumaru et al., 2000; Inumaru et al., 2004) Herein, the octyl group grafted γ-$Al_2O_3$ nanofibers were used to adsorb the 4-nonylphenol highly diluted in aqueous solution. For instance, 50 mg of a sorbent was loaded in a glass column with diameter of 30 mm. 50 mL of aqueous solution

with 4-nonylphenol concentration of 2 ppm by mass, passed through the sorbent bed at a high flow rate of 10 mL/min. As shown in Fig. 8, the parent nanofibers can only remove 15% of the trace 4-nonylphenol molecules in 50 mL water which passed through the sorbent bed within 5 min. In contrast, the octyl grafted samples, C8-FA(s)-1 and C8-FA(S)-2, almost completely removed the toxic 4-nonylphenol under the same conditions. This indicates that the grafted γ-$Al_2O_3$ nanofibers can work under high water flux, which is more feasible for practical application.

**(Fig. 7 -** The profile of water droplets on parent (a) and octyl group grafted small γ-$Al_2O_3$ nanofibers (C8-FA(S)-1) (b).)

(**Fig. 8 -** Removal of 4-nonylphenol in water by parent and octyl group grafted small γ-$Al_2O_3$ nanofibers.)

**4. Discussion**

An important feature of this study is that we grafted functional groups on the external surface of inorganic substrate, γ-$Al_2O_3$ nanofibers. These functionalized nanofibers exhibited high sorption ability for pollutants from water, especially at a high flux. This novel design strategy provided two superior advantages for the fibrous sorbents in practical application. Firstly, the unique fibrous morphology of the inorganic permits large flux passing through the filtration bed and leads to high sorption efficiency because the functional groups are grafted on the external surface of the nanofibers rather than on the internal pore walls of conventional porous supports (Fig. 9b). Undoubtedly these functional groups are readily accessed by the toxic contaminants. This overcomes the problems of the existing sorbents and will greatly facilitate the application of sorption techniques. Secondly, the interconnected voids between fibers, large void size and surface/volume ratio (Yoon et al., 2008), are unique structural features of the nanofibers and are crucial for the superior sorption performance of the fibrous sorbents (Fig. 9a). Fine

powder of γ-$Al_2O_3$ particles with irregular or spherical shapes cannot form structures with both large interconnected voids between particles and large specific surface area, and thus are not as good substrates as the nanofibers for efficient sorbents (Pu et al., 2004). With these unique structural features, the fibrous sorbents are able to achieve high sorption efficiency for the removal of contaminants at large fluxes. This is a valuable property for industrial application of the sorption technique.

(**Fig. 9 -** The schematic diagrams of (a) irregularly aggregated functionalized γ-$Al_2O_3$ nanofibers and (b) a single functional group grafted γ-$Al_2O_3$ nanofiber.)

**5. Conclusion**

γ-$Al_2O_3$ nanofibers provide us with an important opportunity to fabricate efficient and selective sorbents by grafting functional groups on the external surface of the fibers, because they have high surface area, large void size and surface/volume ratio. For instance, thiol and octyl groups can be grafted on the nanofibers by reacting the fibers with thiol- and octyl-silane coupling agents, respectively. The thiol groups grafted nanofibers were employed to adsorb heavy metal ions ($Pb^{2+}$ and $Cd^{2+}$) from water. It was found that the functionalized nanofibers have high sorption capacities and can remove the toxic heavy metals at high fluxes and selectively. The octyl group grafted nanofibers displayed super hydrophobicity (CA = 145 ± 2º) and could efficiently adsorb highly diluted hydrophobic 4-nonylphenol from aqueous solution. The superior sorption efficiency is attributed to unique structural features of fibrous inorganic support. Firstly, the functional groups are grafted on the external surface of the fibers, which can improve the accessibility of the sorption sites to the adsorbates. The other advantageous feature is from the numerous large interconnected voids formed in the aggregation of the randomly oriented nanofibers, which assure that the contaminated solution flows through the sorption bed easily. Actually, the strategy demonstrated specifically for using γ-$Al_2O_3$ nanofibers to improve the accessibility has a much broader significance since it could be applied to address the problem of diffusion difficulties

which seriously affects numerous sorption (and catalysis) process and develop next generation of sorbents and catalysts with better performance.

**Acknowledgement.** This research is supported by the Australian Research Council (ARC).

**References**


Antochshuk, V., Olkhovyk, O., Jaroniec, M., Park, I-S., Ryoo, R, 2003. Benzoylthiourea-modified mesoporous silica for mercury(II) removal. Langmuir 19, 3031-3034.

Behrens, E. A., Sylvester, P., Clearfield, A, 1998. Assessment of a sodium nonatitanate and pharmacosiderite-type ion exchangers for strontium and cesium removal from DOE waste simulants. Environ. Sci. Technol. 32, 101-107.

Brown, J., Mercier, L., Pinnavaia, T. J., 1999. Selective adsorption of $Hg^{2+}$ by thiol-functionalized nanoporous silica. Chem. Common. 69-70.

Bugosh, J. Colloidal alumina -the chemistry and morphology of colloidal boehmite. J. Phys. Chem. **1961**, 66, 1789-1793.

Celis, R., Hermosin, M. C., Cornejo, J., 2000. Heavy metal adsorption by functionalized clays. Environ. Sci. Technol. 34, 4593-4599.

Clifford, D., Subramonian, S., Sorg, T. J., 1986. Water treatment processes. III. Removing dissolved inorganic contaminants from water. Environ. Sci. Technol. 20, 1072-1080.

Cody, C. A., Kemnetz, S. J., 1997. U.S. Patent 5,667,694.

Farmer, V. C., 1974. The infrared spectra of minerals; Mineralogical Society: London.

Feng, X., Fryxell, G. E., Wang, L.-Q., Kim, A. Y., Liu, J., Kemner, K. M., 1997. Functionalized monolayers on ordered mesoporous supports. Science 276, 923-926.

Gadsden, J. A., 1975. Infrared spectra of minerals and related inorganic compounds, Butterworth: London, **1975**.

Greco, C. C., 1996. U.S. Patent 5,512,526.

Gregg, S. J., Sing, K. S. W., 1982. Adsorption, Surface Area and Porosity, 2nd ed.; Academic Press: New York.

Haderlein, S.B., Weissmahr, K.W., Schwarzenbach, R.P., 1996. Specific adsorption of nitroaromatic explosives and pesticides to clay minerals. Environ. Sci. Technol. 30, 612-622.

Huang, C. P., Vane, L. M., 1989. Enhancing As(V) removal by a Fe(II)-treated activated carbon. J. Water Pollut. Control Fed. 61, 1596-1603.

Inumaru, K., Kiyoto, J., Yamanaka, S., 2000. Molecular selective adsorption of nonylphenol in aqueous solution by organo-functionalized mesoporous silica. Chem. Commun. 903-904.

Inumaru, K., Inoue, Y., Kakii, S., Nakano, T., Yamanaka, S., 2004. Molecular selective adsorption of dilute alkylphenols and alkylanilines from water by alkyl-grafted MCM-41: tunability of the cooperative organic–inorganic function in the nanostructure. Phys. Chem. Chem. Phys. 6, 3133-3139.

Komarneni, S., Roy, R. A., 1988. Cesium-selective ion sieve made by topotactic leaching of phlogopite mica. Science 239, 1286-1288.

Lagadic, I. L., Mitchell, M. K., Payne, B. D., 2001. Highly effective adsorption of heavy metal ions by a thiol-functionalized magnesium phyllosilicate clay. Environ. Sci. Technol. 35, 984-990.

Liu, A. M., Hidajat, K., Kawi, S., Zhao, D. Y., 2000. A new class of hybrid mesoporous materials with functionalized organic monolayers for selective adsorption of heavy metal ions. Chem. Common. 1145-1146.

Liu, J., Feng, X., Fryxell, G. E., Wang, L.-Q., Kim, A. Y., Gong, M., 1998. Hybrid mesoporous materials with functionalized monolayers. Adv. Mater. 10, 161-165.

Mercier, L., Pinnavaia, T. J., 1997. Access in mesoporous materials: advantages of adsorbent for environmental remediation. Adv. Mater. 9, 500-503.

Mercier, L., Pinnavaia, T. J., 1998. A functionalized porous clay heterostructure for heavy metal ion ($Hg^{2+}$) trapping. Micro. Meso. Mater. 20, 101-106.

MuÜller, S., Schlatter, C., 1998. Estrogenic potency of nonylphenol in vivo – a case study to evaluate the relevance of human non-occupational exposure. Pure Appl. Chem. 70, 1847-1853.

Nyman, M., Tripathi, A., Parise, J. B., Maxwell, R. S., Harrison, W. T. A., Nenoff, T. M., 2001. A new family of octahedral molecular sieves: sodium $Ti/Zr^{IV}$ niobates. J. Am. Chem. Soc. 123, 1529-1530.

Preziosi, P., 1998. Endocrine disrupters as environmental signalers: an Introduction. Pure Appl. Chem. 70, 1617-1631.

Pu, X., Jiang, Z., Hu, B., Wang, H., 2004. γ-MPTMS modified nanometer-sized alumina micro-column separation and preconcentration of trace amounts of Hg, Cu, Au and Pd in biological, environmental and geological samples and their determination by inductively coupled plasma mass spectrometry. J. Anal. At. Spectrom., 19, 984-989.

Shen, S. C., Chen, Q., Chow, P. S., Tan, G. H., Zeng, X. T., Wang, Z., Tan, R. B. H., 2007. Steam-assisted solid wet-gel synthesis of high-quality nanorods of boehmite and alumina. J. Phys. Chem. C 111, 700-707.

Shimojima, A., Kuroda, K., 2003. Direct formation of mesostructured silica-Based hybrids from novel siloxane oligomers with long alkyl chains. Angew. Chem., Int. Ed. 42, 4057.

Tyler, C.R., Routledge, E.J., 1998. Oestrogenic effects in fish in English rivers with evidence of their causation. Pure Appl. Chem. 70, 1795-1804.

Weng, C. H., Wang, J. H., Huang, C. P., 1997. Adsorption of Cr(VI) onto $TiO_2$ from dilute aqueous solutions. Water Sci. Technol. 35(7), 55-62.

Xia, Y., Yang, P., Sun, Y., Wu, Y., Mayers, B., Gates, B., Yin, Y., Kim, F., Yan, H., 2003. One-dimensional nanostructures: synthesis, characterization, and applications. Adv. Mater. **2003**, 15, 353-389.

Yoon, K., Hsiao, B. S., Chu, B., 2008. Functional nanofibers for environmental applications. J. Mater. Chem. 18, 5326-5334.

Yoshitake, H., Yokoi, T., Tatsumi, T., 2003. Adsorption behavior of arsenate at transition metal cations captured by amino-functionalized mesoporous silica Chem. Mater. 15, 1713-1721.

Zhu, H. Y., Gao, X. P., Lan, Y., Song, D. Y., Xi, Y. X., Zhao, J. C., 2004. Hydrogen titanate nanofibers covered with anatase nanocrystals: a delicate structure achieved by the wet chemistry reaction of the titanate nanofibers. J. Am. Chem. Soc. 126, 8380-8381.

Zhu, H. Y., Riches, J. D., Barry, J. C., 2002. γ-Alumina nanofibers prepared from aluminum hydrate with poly(ethylene oxide) surfactant. Chem. Mater. 14, 2086-4093.

Zhu, H. Y., Gao, X. P., Song, D. Y., Bai, Y. Q., Ringer, S. P., Gao, Z., Xi, Y. X., Martens, W., Riches, J. D., Frost, R. L., 2004. Growth of boehmite nanofibers by assembling nanoparticles with surfactant micelles. J. Phys. Chem. B 108, 4245-4247.

***Table 1.*** The distribution coefficient $K_d$ (mL/g) in the presence and absence of $Na^+$ or $Ca^{2+}$ ions

| Sample | $C_{pb}^{2+}$ (5ppm) | | | $C_{Cd}^{2+}$ (2ppm) | | |
|---|---|---|---|---|---|---|
| | No $Na^+$ or $Ca^{2+}$ ions | $C_{Na}^{+}$ 2000 ppm | $C_{Ca}^{2+}$ 2000 ppm | No $Na^+$ or $Ca^{2+}$ ion | $C_{Na}^{+}$ 2000 ppm | $C_{Ca}^{2+}$ 2000 ppm |
| FA(S) | 10000 | 14000 | 12000 | 4200 | 2600 | 3100 |
| SH-FA(S)-1 | $>5\bullet10^5$ | $>5\bullet10^5$ | $>5\bullet10^5$ | $>5\bullet10^5$ | $>5\bullet10^5$ | $>5\bullet10^5$ |
| SH-FA(S)-2 | $>5\bullet10^5$ | $>5\bullet10^5$ | $>5\bullet10^5$ | $>5\bullet10^5$ | $>5\bullet10^5$ | $>5\bullet10^5$ |
| FA(L) | 4000 | 4700 | 4100 | 3000 | 940 | 1200 |
| SH-FA(L)-1 | 50000 | 55000 | 52000 | $>2\bullet10^5$ | 28000 | $>2\bullet10^5$ |
| SH-FA(L)-2 | 65000 | 68000 | 64000 | $>2\bullet10^5$ | 33000 | $>2\bullet10^5$ |

**Figure 1**

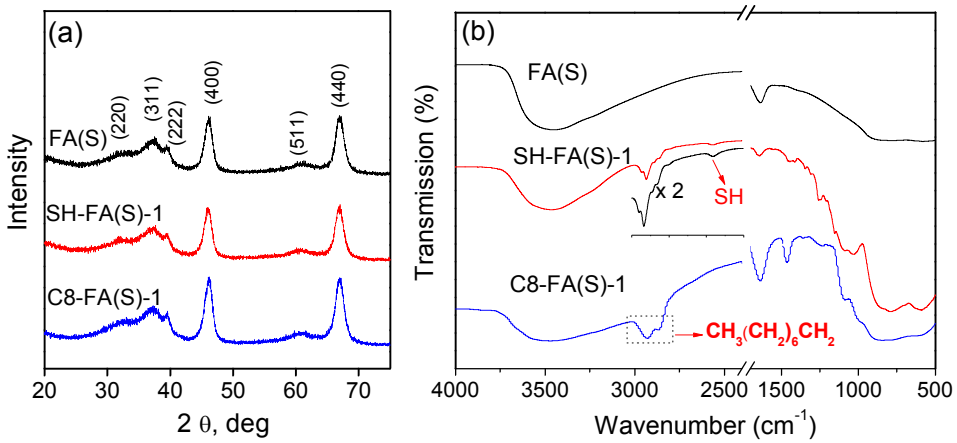


**Fig. 1 -** XRD patterns (a) and FTIR spectra (b) of the parent and functional group (thiol or octyl) grafted small γ-$Al_2O_3$ nanofibers.

Figure 2

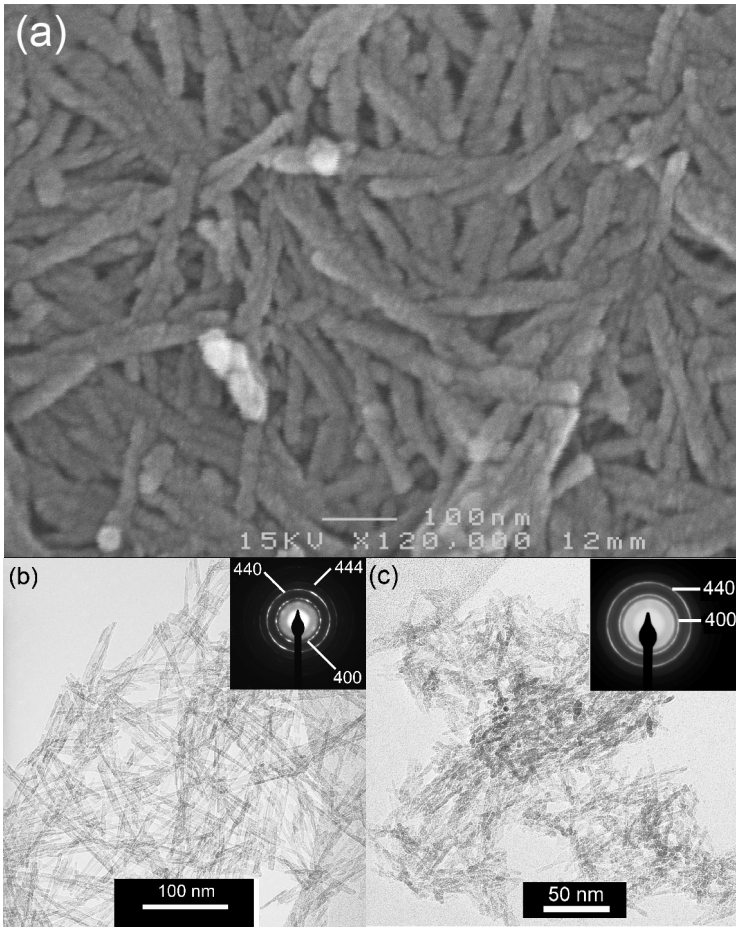


**Fig. 2 -** SEM images of SH-FA(L)-1 (a). The observed width of the fibers is larger than the real width because the sample was coated with a layer of gold (~5 nm thick) for the SEM measurement. TEM image of SH-FA(L)-1 (b) and C8-FA(S)-1 (c). Inset: electron diffraction patterns (EDP) of SH-FA(L)-1 and C8-FA(S)-1.

**Figure 3**

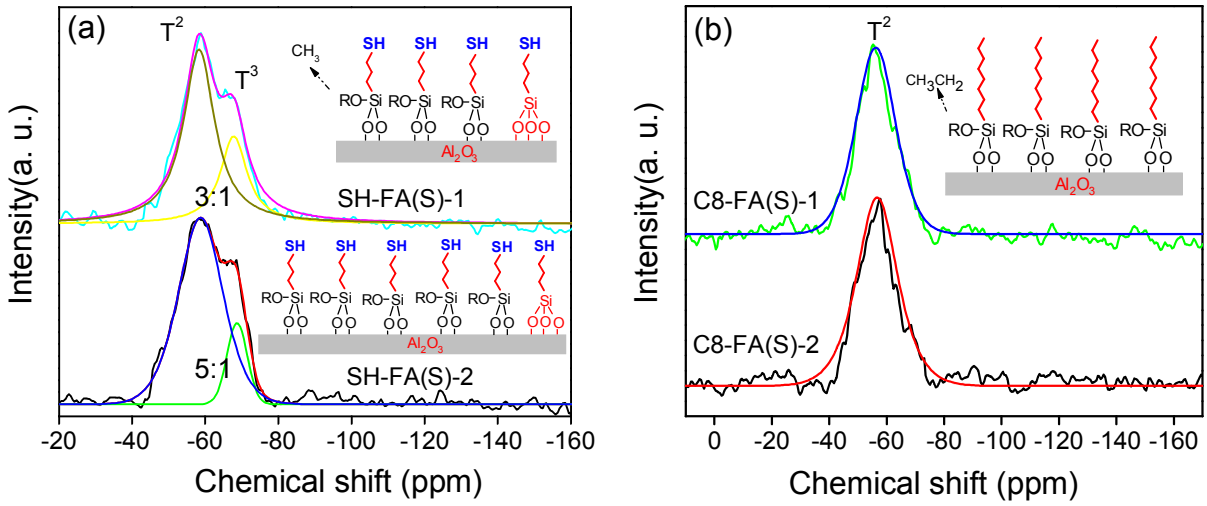


**Fig. 3 -** Solid-state $^{29}$Si MAS NMR spectra of thiol (a) and octyl (b) grafted small γ-$Al_2O_3$ nanofibers. Inset: schematic conformations of functionalized layers on the surface of γ-$Al_2O_3$ nanofibers under different conditions.

**Figure 4**

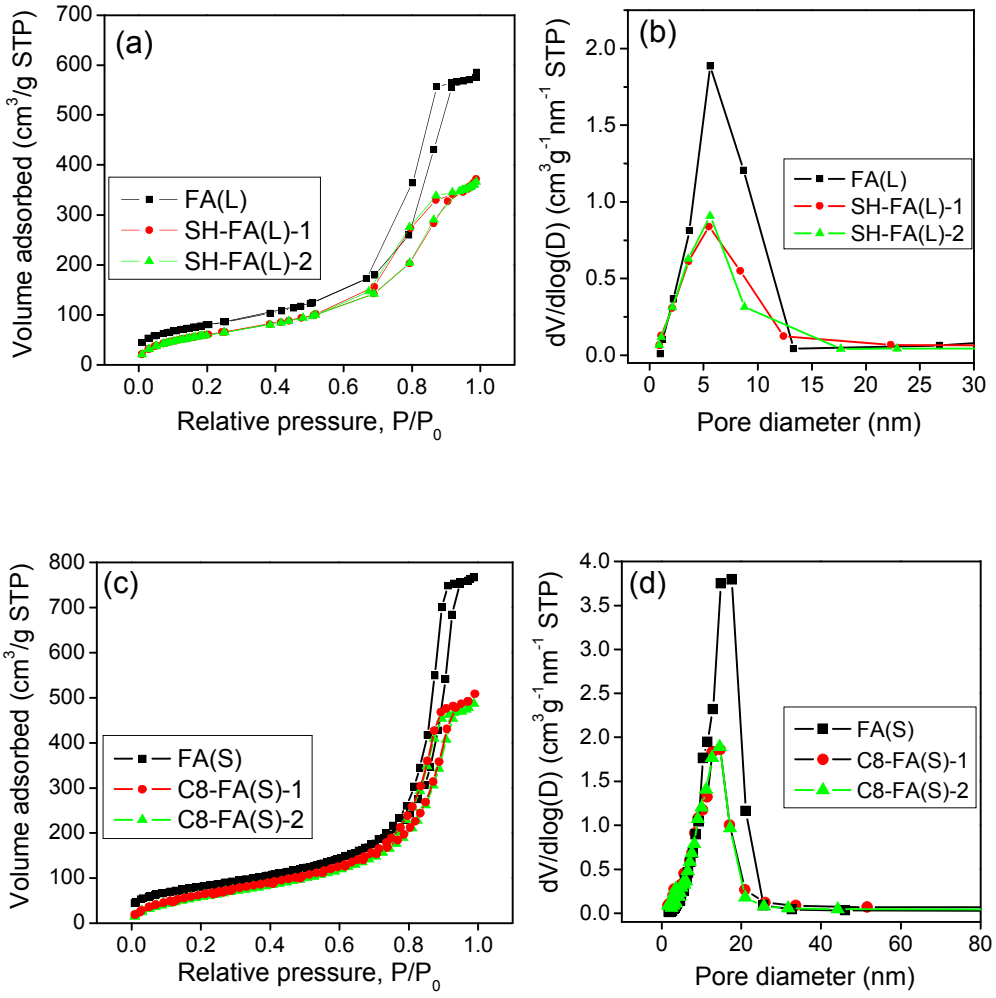


**Fig. 4 -** Nitrogen sorption isotherms (a, c) and pore size distributions (b, d) based on the BJH model for thiol grafted large γ-$Al_2O_3$ nanofibers and octyl grafted small γ-$Al_2O_3$ nanofibers.

**Figure 5**

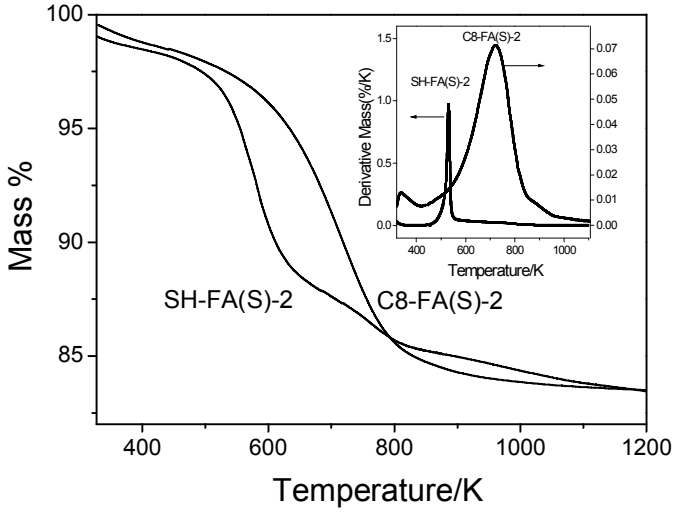


**Fig. 5 -** TGA and DSC (inset) curves of SH-FA(S)-2 and C8-FA(S)-2.

**Figure 6**

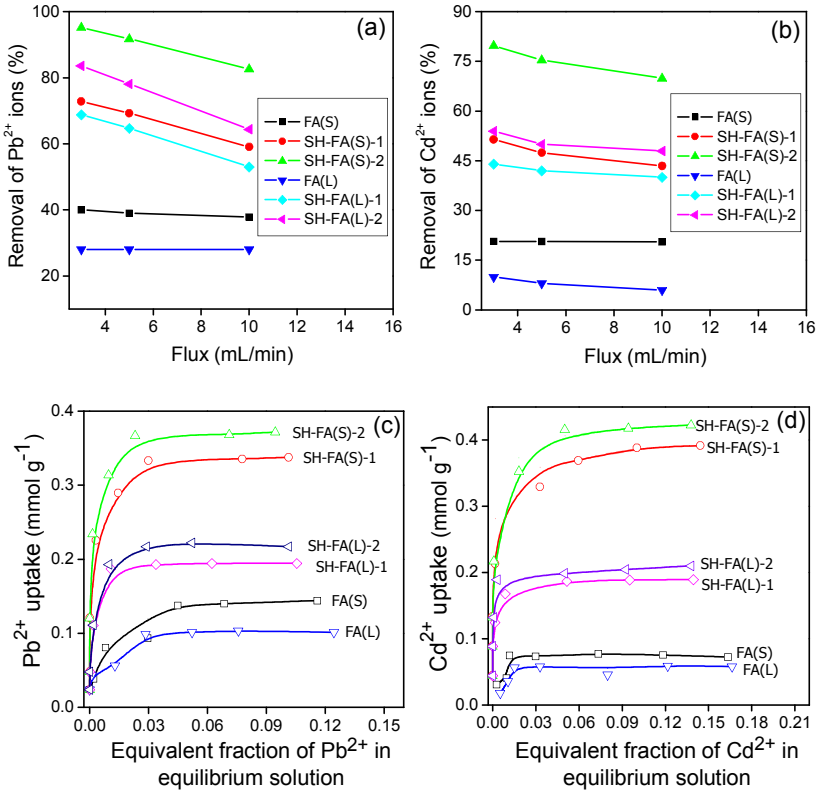


**Fig. 6 -** The performance and equilibrium sorption isotherms of thiol group grafted γ-$Al_2O_3$ nanofibers for removal $Pb^{2+}$ (a, c) and $Cd^{2+}$ ions (b, d) from aqueous solution. Sorption amounts were measured after a suspension of 10 mg of sorbent in 50 ml of $Pb^{2+}$ (or $Cd^{2+}$) solution was shaken at room temperature for 18 h. The concentration range of $Pb^{2+}$ is between 0 to 35 ppm, and that of $Cd^{2+}$ is between 0 to 25 ppm. For comparison, the sorption of the parent γ-$Al_2O_3$ nanofibers were also given.

Figure 7

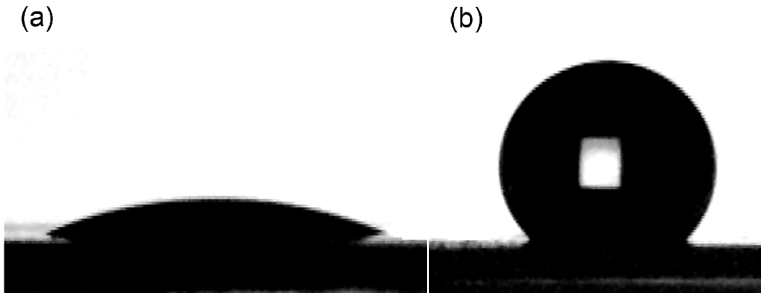


**Fig. 7 -** The profile of water droplets on parent (a) and octyl group grafted small γ-$Al_2O_3$ nanofibers (C8-FA(S)-1) (b).

**Figure 8**

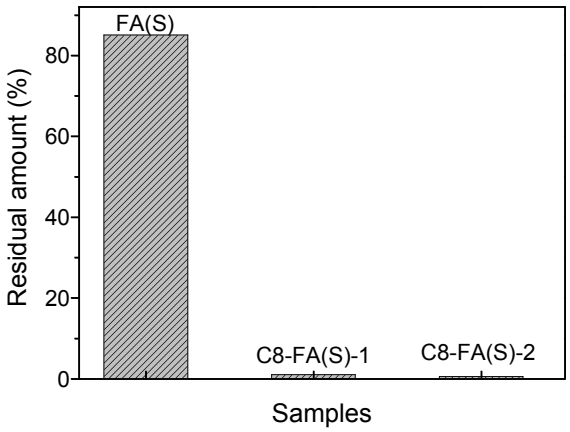


**Fig. 8 -** Removal of 4-nonylphenol in water by parent and octyl group grafted small γ-$Al_2O_3$ nanofibers.

Figure 9

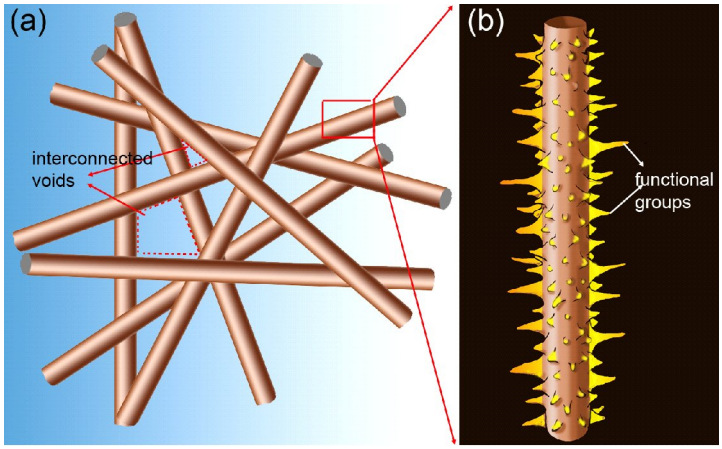


**Fig. 9 -** The schematic diagrams of (a) irregularly aggregated functionalized γ-$Al_2O_3$ nanofibers and (b) a single functional group grafted γ-$Al_2O_3$ nanofiber.